Numerical Study of Electrical Stimulation for Neuronal Cell Growth on Silica Aerogel Substrate

Sakib Al Soyeb [a], Bashir I. Morshed [a], and Firouzeh Sabri [b]
[a] Department of Electrical and Computer Engineering, The University of Memphis, Memphis, TN 38152
[b] Department of Physics, The University of Memphis, Memphis, TN 38152

***Abstract*- An aerogel-based Neuronal Printed Circuit Board (NPCB) with electrical stimulation capabilities is currently under investigation as an alternative method for repair of injury sustained to peripheral nerves. Here, we report the results of the numerical analysis of electric field distribution, fluidic motion, and temperature rise due to such superficial electrical stimuli. In this analysis, a cylindrical aerogel structure is modeled for both voltage and current stimulation using COMSOL finite element analysis software. Voltage excitation of 100 mV and current excitations of 0.1 to 1 A are applied to a pair or a single electrode of gold track with dimension of 20×2×0.2 mm^3. Simulation results demonstrate that electric field lines are highly concentrated on the surface of the aerogel where the gold tracks exist. Besides, the stimulation generates fluidic motion, and the steady state temperature increase due to the stimulation is less than 1K for current stimulation of less than 0.35 A.**

Keywords—Aerogel, electric field, finite element analysis, neuronal stimulation.

I. Introduction

Repair of severed or injured peripheral nerves is a necessary to restore complete functionality of involved muscle groups. Existing technology for peripheral nerve repair mostly consist of passive devices that bridge the proximal and distal ends of severed nerves. These consist of guidance channels and conduits that lack electrical stimulation capabilities even though neurons are known to respond to electrical stimulations [1]. Several theories have been suggested to explain the effect of electric stimulation on nerve regeneration These include (*i*) electrophoretic redistribution of cell membrane growth factor and adhesion receptors or cytoskeletal proteins such as actin, all of which are involved in growth cone migration, (*ii*) favorable membrane or extracellular matrix protein conformational changes, (*iii*) direct hyperpolarization or depolarization of nerves, (*iv*) enhancement of protein synthesis, and (*v*) field-induced gradients of ions and molecules in the culture medium or tissue fluid [2]. It has been demonstrated previously that recovery of severed nerves is improved and enhanced by providing directional cues and electrical stimulation that increased the sciatic nerve and PC12 cell regeneration rates without any significant change in cell viability, pH, and temperature [3-5].

Polyurea crosslinked silica aerogels are particularly interesting materials for applications relating to active nerve repair devices due to their mechanical strength, high degree of porosity, and electrical insulation. Studies have suggested the biocompatibility of this material both *in vivo* and *in vitro* [6,7].

In this paper, the numerical study of electric potential distribution, fluidic flow, and thermal effect due to electrical excitation gold tracks on aerogel substrate is presented.

II. Simulation Setup

In a stationary coordinate system, the point form of Ohm's law is given by [8]

$$J = \sigma E + J^e \quad (1)$$

where J is the resultant current density in the medium, σ is the electrical conductivity of the medium, E is the electric field, and J^e is the externally generated current density. The static form of the equation of continuity can be expressed as:

$$\nabla . J = -\nabla \cdot (\sigma \nabla V - J^{e)} = 0 \quad (2)$$

For current sources, this expression can be generalized to:

$$-\nabla .(\sigma \nabla V - J^e) = Q_j \quad (3)$$

where Q_j is the current source. The numerical simulation tool solves the following equation where d is the thickness in the z direction:

$$-\nabla .d(\sigma \nabla V - J^e) = dQ_j \quad (4)$$

COMSOL Multiphysics finite element analysis (FEA) software version 4.2a (COMSOL Inc., Burlington, MA, USA) was used for this numerical study. The model, shown in Figure 1, composes of a cylindrical aerogel substrate of 6 mm radius with 5 mm height suspended inside 40 mm^3 water-cube simulation box. For current simulation, a single gold track, while for voltage simulation, a pair of gold tracks was placed on the top surface (z-axis) of the cylindrical aerogel. The dimension of each gold track is 20×2×0.2 mm^3, while the pair of electrodes is spaced by 5 mm. Simulation temperature was set to 293^{0}K, with electric currents (ec) and laminar flow (spf) physics (as well as electrothermal physics, where appropriate) of COMSOL enabled. The relevant parameters used in the FEA simulation are given in Table 1 [8,9].

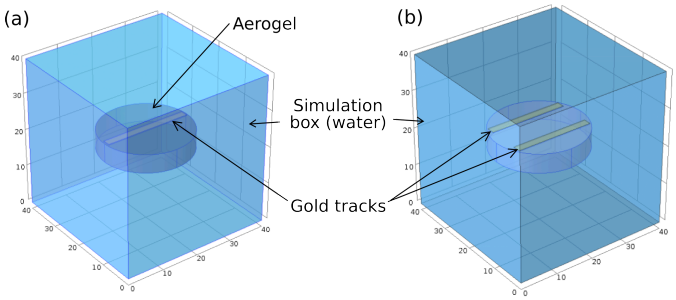

Fig. 1. Models used for simulations: (a) Current excitation model with one gold track on an aerogel substrate, and (b) Voltage excitation model with a pair of gold tracks on an aerogel substrate. [Length unit: μm]

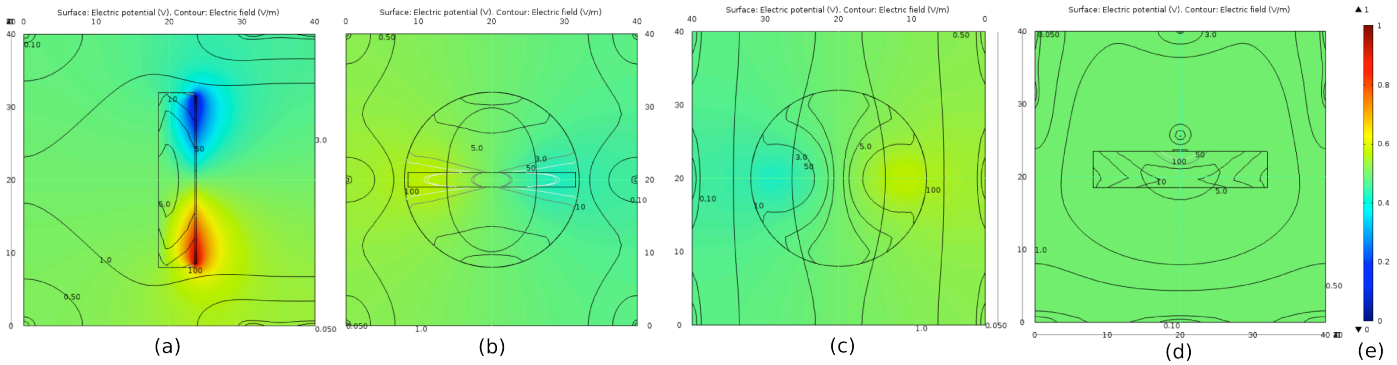

Fig. 2. Electric potential (surface plot) and electric field (contour plot) distributions for current excitation. (a) Cross sectional view along the track. (b) Top view. (c) Bottom view. (d) Cross sectional view perpendicular to the track. (e) Color scale. [Units: Electric potential – V, Electric field – V/m.]

TABLE I: PARAMETERS USED IN THE NUMERICAL SIMULATIONS

Material	Parameter	Value	Unit
Water	Relative permittivity	80.1	-
	Electric conductivity	$5.5x10^{-6}$	S/m
Gold	Relative permittivity	0	-
	Electric conductivity	$1.278x10^{12}$	S/m
Aerogel	Relative permittivity	3.2	-
	Electric conductivity	$1x10^{-18}$	S/m
Polypropylene	Relative permittivity	2.28	-
	Electric conductivity	$1x10^{-18}$	S/m

Boundary conditions were set to insulation for outer boundaries, while continuity for internal boundaries. Fluidic simulation domain was limited to water. Extremely fine mesh sizes were auto generated by "Physics-controlled mesh" of COMSOL. For current excitation, 0.1 mA, 10 mA and 1 A were applied to a terminal of the gold track while the other terminal was grounded. For voltage excitation, 100 mV was applied to the top surface of one track while the other track was grounded. Mesh option was selected as "Physics controlled extremely fine".

III. SIMULATION RESULTS

Figure 2 shows the results of electric potential and electric field distributions for current excitation. The terminals show the maximum electric potentials, while the electric field above the aerogel is higher than that on the bottom (Figure 2a). The potential and electric field distribution are slightly asymmetric above and below the gold tracks. High electric field contours (eg. 100 V/m) on the surface of the gold track are noted (Figure 2b), while the relatively low electric field lines on bottom (Figure 2c). Figure 3 depicts fluidic velocity magnitude and fields, which maximizes at edges of the gold track. Figure 4 shows the simulation results of electric potential and electric field distribution for voltage excitation. Similar to the current excitation, the potential and electric field distribution are higher on the top surface and slightly asymmetric. Figure 5 presents fluidic velocity magnitudes and fields.

Figure 6 depicts the simulation results of Joule heat distribution for current excitation. For convection cooling heat transfer coefficient 20 W/(m^2-k) is used. The temperature remains unchanged at lower current setting used (0.01 A). For a change of 1^0K, 2^0K and 10^0K from initial temperature (293^0K), the required current was 0.35, 0.5 and 1.12 A, respectively. Figure 7 shows the results of temperature distributions for voltage excitation of 100 mV. The terminals show the maximum temperature, while the temperature above the aerogel is higher than that on the bottom (Figure 7b).

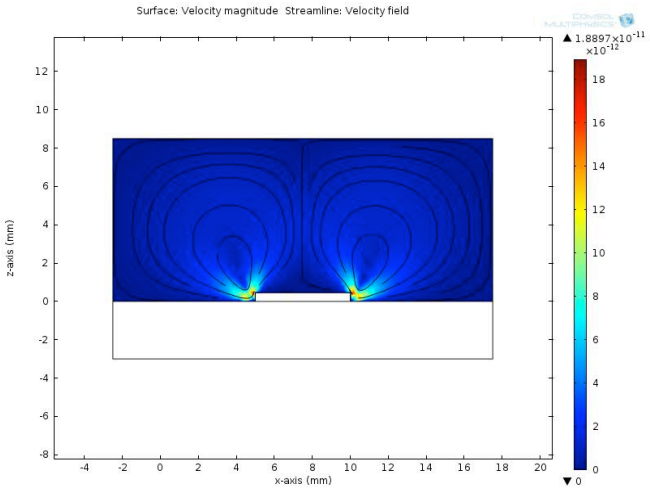

Fig. 3. Fluidic velocity magnitude and velocity field due to the current excitation (cross sectional view perpendicular to the track).

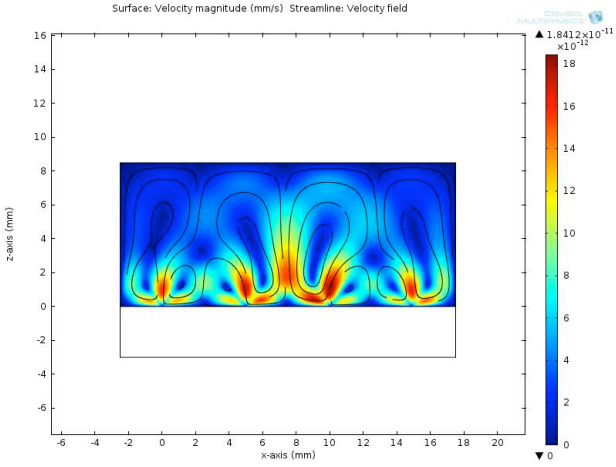

Fig. 5. Fluidic velocity magnitude and velocity field due to the voltage excitation (cross sectional view perpendicular to the tracks).

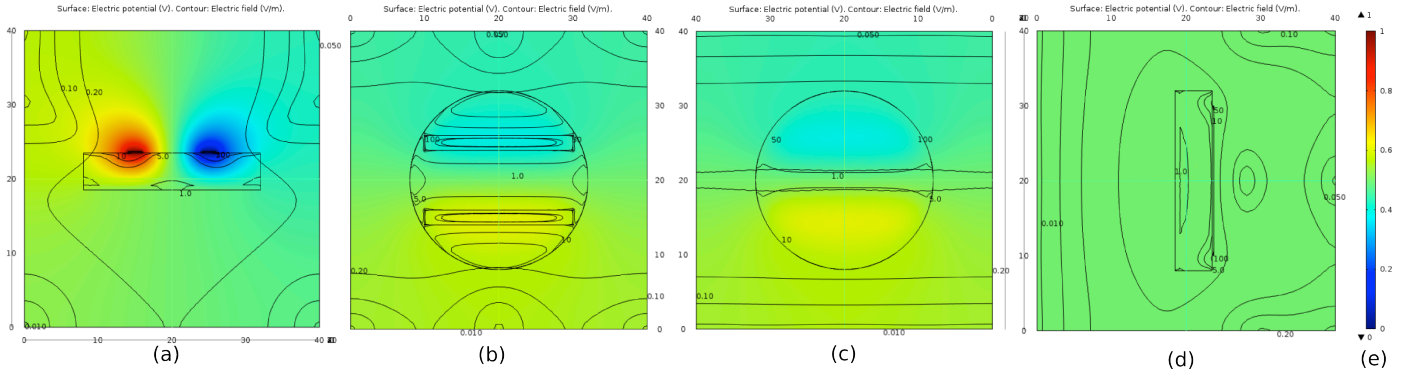

Fig. 4. Electric potential (surface plot) and electric field (contour plot) distributions for voltage excitation. (a) Cross sectional view perpendicular to the tracks. (b) Top view. (c) Bottom view. (d) Cross sectional view in the middle of the tracks. (e) Color scale. [Units: Electric potential – V, Electric field – V/m.

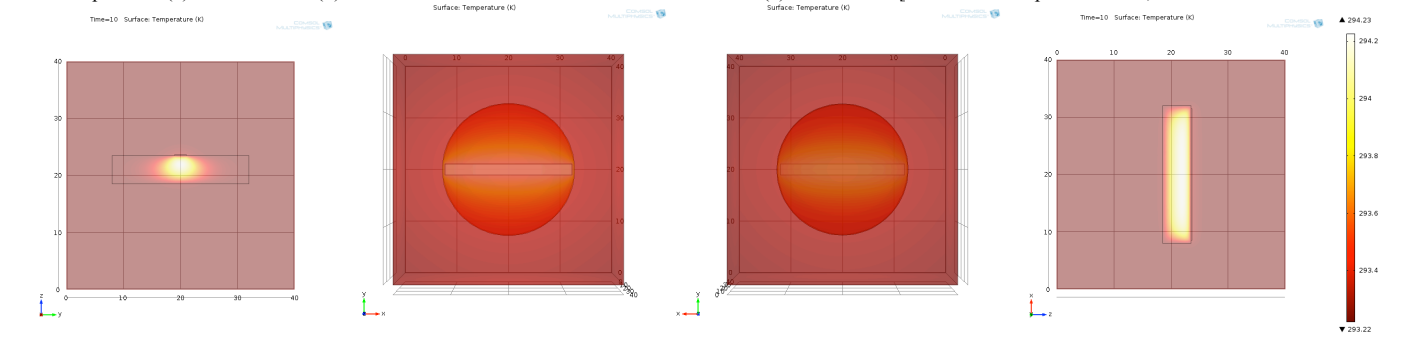

Fig. 7. Joule heating distribution due to the voltage excitation of 100 mV. (a) Cross sectional view perpendicular to the tracks. (b) Top view. (c) Bottom view. (d) Cross sectional view in the middle of the tracks. (e) Color scale. [Units: Electric potential – V, Electric field – V/m.]

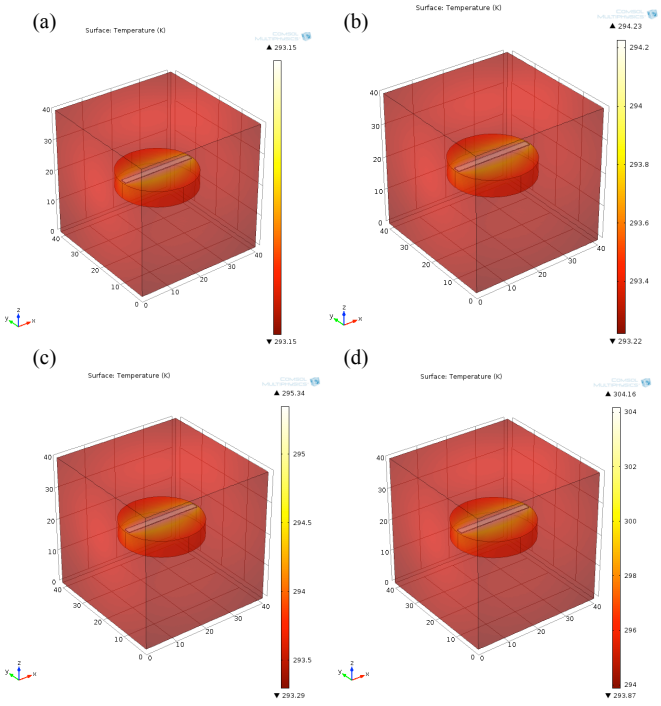

Fig.6. Joule heating distribution due to the current excitation. (a) Temperature change is insignificant at 0.01 A. (b) 1^0 k increased temperature at 0.35 A. (c) 2^0 K temperature increase at 0.5 A. (d) 10^0 K temperature increase at 1.12 A. [Units: Electric current – A, Temperature – K.]

As nerve cells are temperature sensitive, an abrupt change of temperature might adversely affect the nerve cell. For example, astrocytoma cells can survive only in specific temperature range. The best incubating temperature is 37°C, while at 40°C astrocytoma cells experience heat shock, and at 42°C they cease to live. These simulations indicate that current excitation with lower than 0.35 A will not cause significant change of temperature for cells to have any adverse effect. Stimulations of 0.5 - 1.12 A will increase temperatures from 2 to 10^0 K which might adversely affect the nerve cells.

Figure 8 depicts surface electric potential due to current excitation, where the maximum voltage drops are across the gold tracks. Precise control of the voltage excitation is required for neuronal stimulation. Inducing such excitation through action potential can be accomplished from appropriate voltage excitation from either the edge or on the gold track. Hence, this is expected to influence the direction of neuron growth perpendicular to the gold tracks on the aerogel.

Figure 9 depicts current density distribution across the gold track. Higher current density is across the source of current while lower near to the ground, indicating the potential influence of neuron growth on the electronic charge might be directed from the ground terminal to the positive terminal.

IV. Conclusion

In this paper we explore electrical stimulation on the growth and directionality of PC12 neuronal cells cultured *in vitro*. As nerve are environment sensitive it is vital to simulate and find

out that electrical and voltage stimulation process does not release excess heat, pressure and fluidic velocity to damage the cells. As these parameters are interdependent without simulation it would be difficult to determine what changes in electrical stimulation influence heat, pressure or fluidic velocity. It could be concluded by simulation that heat, pressure or fluidic velocity produced from electrical and voltage stimulations might not endanger live cells. An aerogel-based Neuronal Printed Circuit Board (NPCB) with electrical stimulation capabilities might be able to influence neuronal growth and directionality. The simulation results show that the higher field distribution to the side of the gold tracks for both current and voltage excitation.

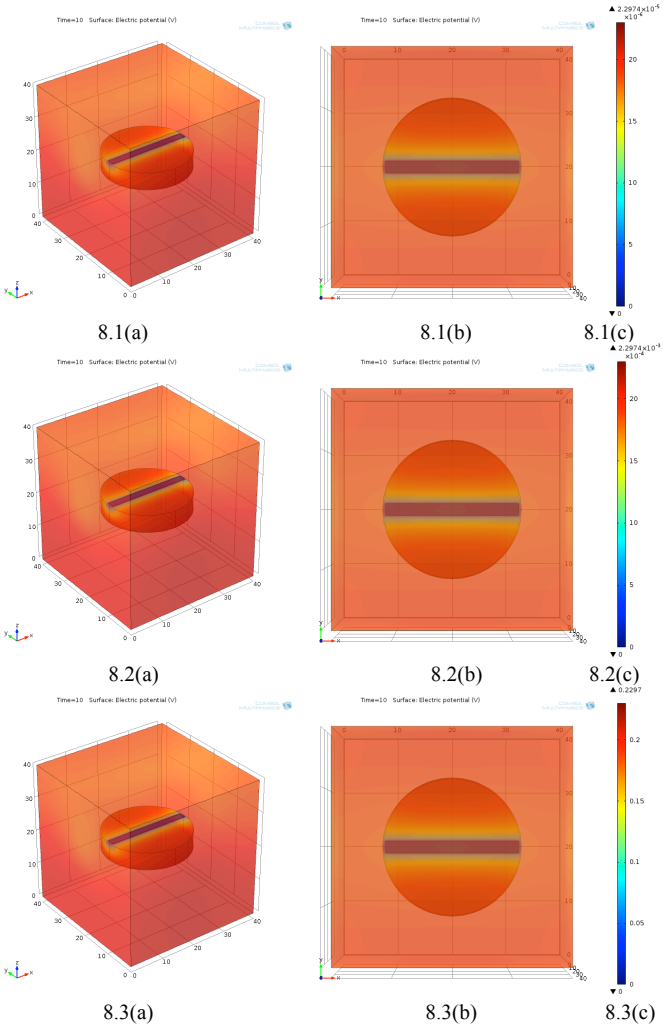

Fig.8. Voltage drop to the current excitation. 8.1(a), 8.2 (a), 8.3(a): Voltage drop in 3D view due to 0.0001 ,0.01, and 1 A current flow, respectively. 8.1(b), 8.2 (b), 8.3(b): Voltage drop in top view due to 0.0001 ,0.01 ,1 A current flow, respectively. 8.1(c), 8.2 (c), 8.3(c) Corresponding voltage distribution scales. [Units: Electric current – A, Electric voltage – V]

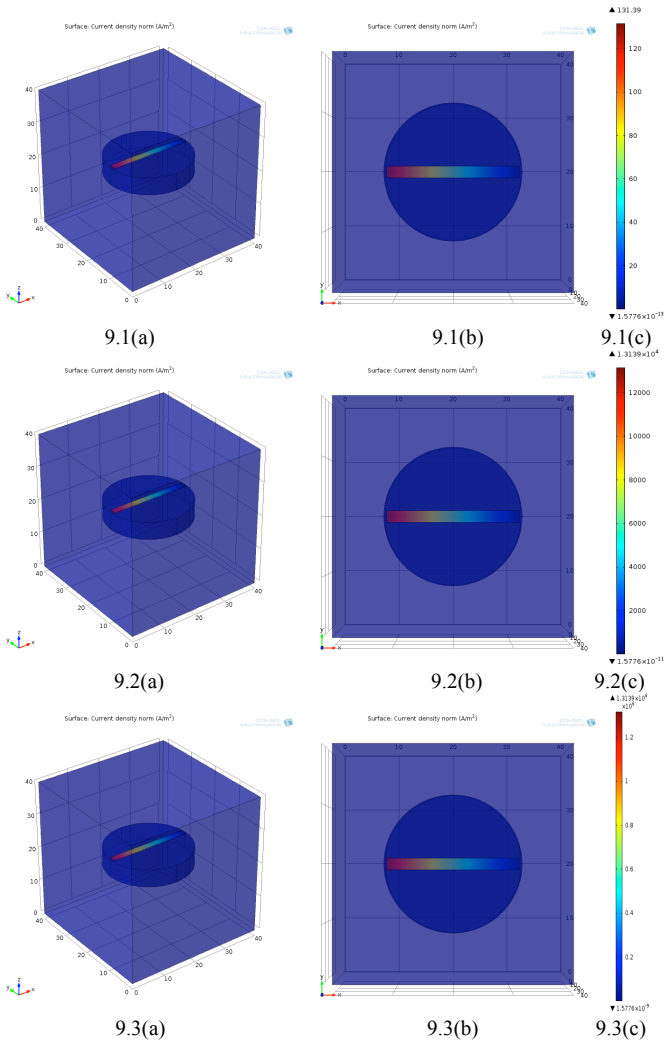

Fig.9. Magnitude of current density due to current excitation. 9.1(a), 9.2(a), 9.3(a): Current densities in 3D view due to 0.0001 ,0.01 ,1 A current flow, respectively. 9.1(b), 9.2 (b), 9.3(b): Current densities in top view. 9.1(c), 9.2 (c), 9.3(c) Corresponding scales. [Units: Current – A, Current density – A/m^2]

REFERENCES

[1] Goldberg JL, "Role of electrical activity in promoting neural repair", *Neuroscience Letters,* vol. 519, pp. 134– 137, 2012.

[2] Schmidt CE, Shastri V, Acanti J, "Stimulation of neurite outgrowth using an electrically conducting polymer", *Nat Acad Sci*, vol. 94, pp. 8948–53,1997.

[3] Ghasemi-Mobarakeh L, Prabhakaran MP, Morshed M, *et al,* "Application of Conductive Polymers, Scaffolds and Electrical Stimulation for Nerve Tissue Engieering," *J Tissue Eng Regen Med*, vol. 5, pp. e17-e35, 2011.

[4] Wan L, Xia R, Ding W, "Short-term low-frequency electrical stimulation enhanced remyelination of injured peripheral nerves by inducing the promyelination effect of brain-derived neurotrophic factor on Schwann cell polarization," *J Neurosci Res*, vol. 88, no. 12, pp. 2578-2587, 2010.

[5] Huang J, Lu L, Zhang J, *et al.* "Electrical stimulation of conductive scaffold promotes axonal regereration and remyelination in a rat model of large nerve defect," *PLoS One*, vol. 7, no. 6, pp. e39526, 2012.

[6] Sabri F, Cole JA, Scarbrough MC, Leventis N, "Investigation of Polyurea-Crosslinked Silica Aerogels as a Neuronal Scaffold: A Pilot Study", *PLoS One*, vol. 7, no. 3, pp. e33242, 2012.

[7] Sabri F, Boughter Jr JD, Gerth D, *et al.* "Histological Evaluation of the Biocompatibility of Polyurea Crosslinked Silica Aerogel Implants in a Rat Model: A Pilot Study", *PLoS ONE*, vol. 7, no. 12, 2012.

[8] Comsol Multiphysics modeling guide. November 2008 ,COMSOL3.5a

[9] Valentini, R. F. (1995) in *The Biomedical Engineering Handbook*, ed. Bronzino, J. D. (CRC, Boca Raton, FL), pp. 1985–1996.